Design and Modeling of Nanocrystalline Iron Core Resonant Transformers for Pulsed Power Applications

Andrew H. Seltzman, Paul D. Nonn and **Jay K. Anderson**
University of Wisconsin - Madison
Department Physics
1150 University Ave
Madison, WI 53706, USA

ABSTRACT

A high power resonant three phase switch mode power supply has been constructed at University of Wisconsin to drive a klystron tube. Utilization of a resonant transformer with loosely coupled secondaries allows generation of high boost ratios exceeding the turns ratio while providing high efficiency. Use of nanocrystalline iron cores provides high volt seconds while maintaining low loss at high switching frequencies. Analytic models are developed and compared to measured data from two different size resonant transformers and effects of turns ratio, load resistance, and primary are examined and compared to theory.

Index Terms — **Resonant power conversion, resonators, HF transformers, voltage transformers, power systems, klystrons, pulse generation, pulse width modulated power converters, pulse width modulated inverters, pulse width modulation, DC-DC power conversion, power conversion, power conversion harmonics**

1 INTRODUCTION

POLYPHASE resonant power converters are a new method to generate high voltages with high power while maintaining a small physical size of 10 times smaller than previous methods. Such power converters are capable of producing 10s of MWs at 100s of kV. Additional benefits include inherent fault tolerance; the power converter must be designed to be matched to a given load such that in the event of a fault, the resonant circuit will be de-Qed thereby preventing power transfer. In the event of an arc fault, the system can safely run through the fault without damage to the load or supply, while the reduction in power transfer may be sufficient to clear the arc fault. Resonant power converters with nanocrystalline iron cores maintain the high permeability of iron cores, while allowing efficient use at higher frequencies in the 10s of kHz usually reserved for ferrite materials. Consequently, a nanocrystalline transformer can provide 300 times the power transfer capability as a 60 Hz transformer for a given size and weight. For comparison, a 100 kV, 60 Hz system carrying 20 A_{rms} and utilizing soft iron cores will be on the scale of 35 tons and have about 30 kW losses while the transformer in a polyphase resonant converter operating at 140 kV and 20 kHz carrying 20 A_{rms} utilizing a nanocrystalline core will weigh 200 kg and have about 3 kW of losses. Efficiency of as high as 97% may be realized with such a system [1]. Such resonant systems can achieve significantly greater power levels with a given set of power electronics in part to the resonant nature of the secondary which allows soft switching thereby reducing junction heating in the IGBTs. Given the exact nature of the system, either zero voltage switching or zero current switching may be utilized by switching the IGBTs during the period of reverse commutation of the anti-parallel diodes in the IGBT module, or by operating near resonance such that the IGBTs switch near the zero crossing period of primary current [2, 3].

The use of resonant circuits in high voltage switching power converters allows the voltage boost ratio of the transformer to exceed the turns ratio, resulting in more compact designs, as shown in Figures 1 and 2, and reduction of copper usage in the secondary winding.

Figure 1. Three phase resonant power supply.

Manuscript received on 30 September 2012, in final form 7 March 2013.

The strong dependence of the boost ratio on switching frequency allows the power supply to regulate output voltage by shifting switching frequency. By switching at full duty cycle near resonance, the primary voltage and current are in phase, allowing for zero current switching (ZCS), and significant reduction of switching losses. As switching frequency moves away from resonance, the IGBT current at the switching events increases from zero, however with only two switching events per cycle, switching losses remain low [4-6].

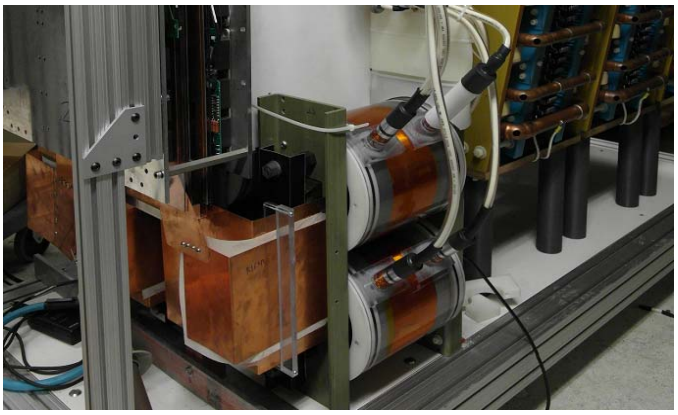

Figure 2. Resonant power supply transformers.

Additional benefits of resonant topologies include the strong dependence of power transfer on a matched output load; in the event of a short circuit, the resonant circuit will be de-Qed and power transfer will automatically reduce without damage to the supply or klystron load [7-10].

The construction of such a power supply required the design of a suitable resonant transformer system utilizing a nanocrystalline core. Initially, a time consuming trial and error approach of transformer design was utilized to find the optimum turns ratio, involving the production of multiple secondaries with varying numbers of turns. Subsequently the data gathered from the multiple transformer designs was used to develop and validate numerical and analytical models of resonant transformers which may be used for future designs.

2 RESONANT TRANSFORMER CHARACERISTICS

In contrast to closely coupled inductive systems, such as a tightly wound transformer with low leakage inductance, loosely coupled transformers provide a high leakage inductance that may be used to form a resonant circuit. In many cases efficient power transfer may only be attained if either or both the primary and secondary windings are capacitively compensated. In closely coupled reactive power systems, the reactive power is usually less than the real power transferred, while in certain loosely coupled systems, the reactive power can be up to 50 times the real power [11]. High leakage inductance is achieved by designing the secondary winding with a large private magnetic flux.

For use in high power density switching power supplies, a core material with high volt seconds and low loss must be used. Soft iron cores have unacceptably high loss due to their large lamination thickness and magnetic properties leading to eddy current and hysteresis losses, respectively. Ferrite cores operate efficiently at high frequency, but saturate at low magnetic flux, limiting the volt seconds per turn that may be carried by the core. The use of nanocrystalline or amorphous cores allows for high saturation flux providing adequate volt seconds per turn for high power density applications while providing low losses at high frequency [12-14].

Resonant transformers for klystron power supply applications have traditionally been designed with a tightly wound, low impedance primary made of either a copper strap winding or Litz wire. The secondary is loosely wound to generate a large private magnetic flux and achieve the necessary leakage inductance. A resonator capacitor is placed in parallel with the secondary and the inductance and capacitance are tuned to achieve the desired resonant frequency and boost ratio.

Further benefits of resonant transformers include reduction of switching harmonics. While a non-resonant transformer will couple higher harmonics from a square wave input into the secondary, a resonant system will only couple them at the turns ratio, while only the fundamental harmonic will be passed at the boost ratio, providing a sinusoidal waveform to the rectifier. This can reduce switching harmonics by a factor of the (boost ratio) / (turns ratio) which is routinely on the order of 10:1.

3 RESONANT TRANSFORMER DESIGN

Two transformer designs are presented, one “large core resonant transformer” for use on the power supply with a 63mm width by 44mm depth core cross section and a 114mm width by 228 mm height window area utilizing a nanocrystalline “Namlite” core, and a “small core resonant transformer” for further testing of analytic models with a 25 mm by 25 mm core cross section and a 100 mm by 100mm window area utilizing an amorphous “Metglas” 2605SA1 core. The small core transformer was tested with both low resistance and high resistance primary windings to evaluate the effect of primary resistance on transformer resonance. Both transformers examined herein have a parallel pair of 10 turn primary windings on each leg of the C-core and a parallel pair of secondaries. All quoted leakage inductance is the inductance of the two secondaries in parallel.

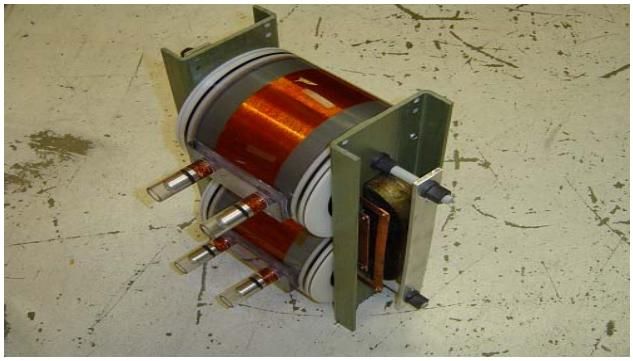

Figure 3. Large core resonant transformer.

3.1 LARGE CORE TRANSFORMER TESTING

A set of three transformers, as shown in Figures 3 and 4, with loosely coupled resonant secondaries are used to drive the klystron tube through a doubling rectifier.

Each transformer is built around a nanocrystalline iron core that allows low loss operation at high switching frequencies while providing a high saturation flux when compared to ferrite materials. The primaries consist of a parallel pair of 10 turn copper strap coils, wound around a polycarbonate form and held in close proximity to the cores. Each winding used a 0.8 mm thick, 12.5 mm wide copper strap, wound in a helical manner around a 6.4 mm thick polycarbonate coil form. The secondaries consist of a parallel pair of 165 mm diameter,136 turn coils made out of 0.68 mm diameter solid enamel coated wire and have a parallel 50 nF capacitor resonator. For added current handling capability, each secondary consists of two layers of wire, connected in parallel at the ends of the windings and separated by Mylar insulation. Individual oil jackets enclose each secondary as shown in Figure 4; providing insulation, cooling and preventing corona discharge on the windings. Further suppression of corona discharge is accomplished by grounding the cores to prevent charge buildup and placing a faraday screen consisting of conductive copper tape on the inside surface of the secondary oil tank to prevent displacement current from the windings from capacitively coupling to the core or surrounding air.

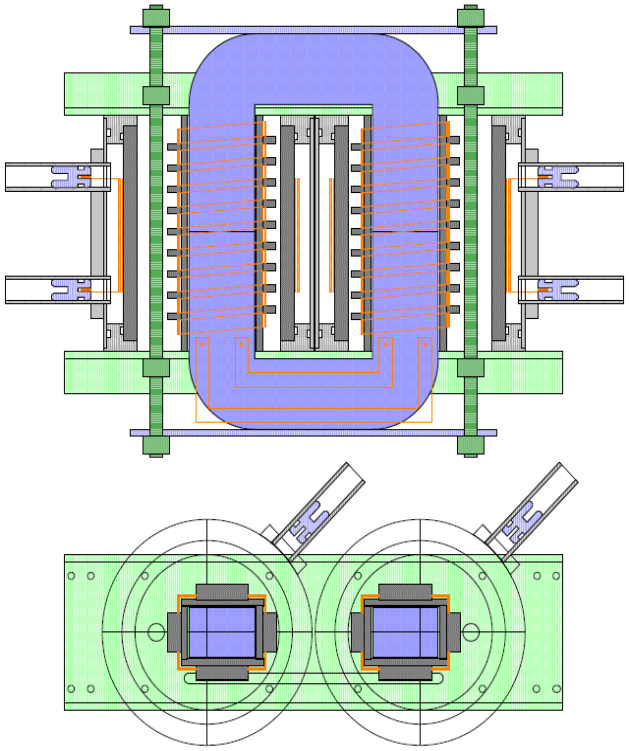

Figure 4. Large core resonant transformer assembly diagram.

The final transformer design was obtained through trial and error, testing secondary windings with 76 through 156 turns until a final design with suitable inductance for the desired resonant frequency and maximum boost ratio was obtained, as shown in Figures 5 and 6.

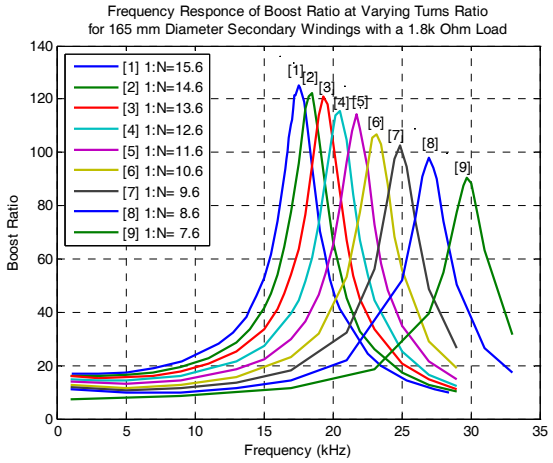

Figure 5. Boost ratio for the large core resonant transformer with a 1.8k ohm load.

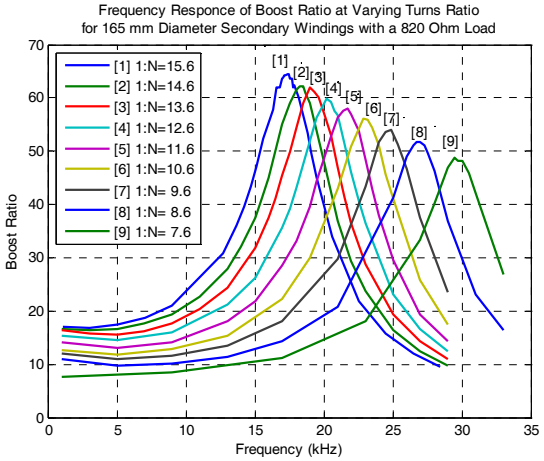

Figure 6. Boost ratio for the large core resonant transformer with an 820 Ω load.

Analytical and numerical models for the transformer's transfer function were derived and compared to measured data. The final version of the transformer was chosen to have a 136 turn secondary, a primary leakage inductance of 8 µH, a primary magnetizing inductance of 1.69 mH, a secondary referred total leakage inductance of 1.36 mH, a primary series resistance of 27.3 mΩ, and a secondary series resistance of 1.2 Ω. A spice model of the transformer is presented in Figure 7.

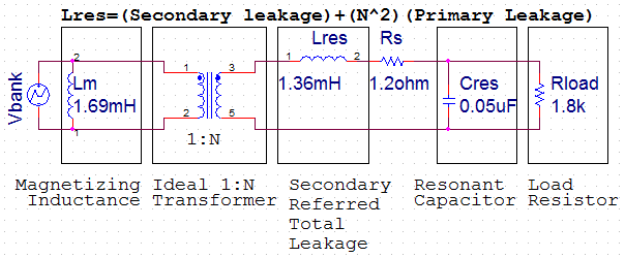

Figure 7. Full transformer model for large core transformer.

A simplified model of the transformer may be obtained by approximating that the magnetizing inductance is infinite, which remains valid as long as the transformers are run without saturating the cores, that primary resistance and leakage inductance is negligible, and that the cores are

magnetically lossless. The system may then be modeled as a resonant LC tank circuit driven by a voltage equal to the primary voltage times the turns ratio as shown in Figure 8.

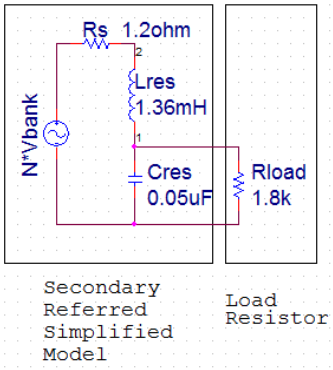

Figure 8. Simplified transformer model for large core transformer.

An analytical model for the inductance of a loosely coupled transformer was obtained by modifying the Wheeler formula for a short solenoid [15] to obtain leakage inductance. Assuming an ideal model of the transformer where magnetic flux is entirely excluded from the core and primary of the transformer when the primary is shorted, the Wheeler formula is modified by subtracting the total core cross sectional area, denoted "Acore", from the cross sectional area of the secondary winding as shown in equation (1) where "r" is coil radius, "h" is coil height, and "Acoil" is coil area.

$$L_{wheeler} = \frac{10\mu_0 N^2 \left(A_{coil} - A_{core}\right)}{\left(9r_{coil} + 10h_{coil}\right)} \quad (1)$$

The resulting formula, called the "Wheeler compensated area" formula herein, predicts the leakage inductance of the transformer with high accuracy when compared to the Wheeler formula without area compensation and the long solenoid approximation as shown in Figure 9.

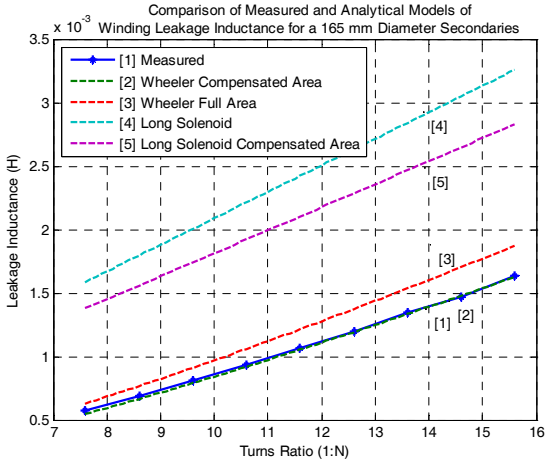

Figure 9. Measured and analytical models of secondary winding leakage inductance for the large core transformer.

An analytical model of the transformer's transfer function was developed and compared to experimental data. The transformer model may be simplified to a secondary referred model consisting of a voltage source of N times the primary voltage connected across a resonant circuit including an inductor of finite ESR with inductance calculated from the Wheeler compensated area formula, and an ideal capacitor with a load resistor connected in parallel across the capacitor as shown in equation (2).

$$\frac{V_{sec}}{V_{pri}} = \frac{N}{\left[1 + \left(R_{inductor} + j\omega L_{res}\right)\left(\frac{1}{R_{load}} + j\omega C_{res}\right)\right]} \quad (2)$$

The resulting transfer function predicts the boost ratio of the transformer over the desired frequency range to reasonable accuracy as shown in Figure 10.

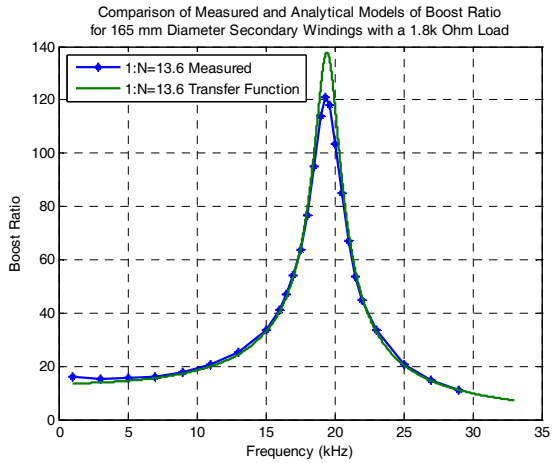

Figure 10. Measured and analytical models of boost ratio for the large core transformer.

The boost ratio at resonance for two different load resistances is shown in Figure 11. As seen in Figure 10, the boost ratio predicted by the analytical formula is consistently higher than the measured values. Note that the model using equation (2) uses the DC resistance of the secondary and does not include skin effects or finite primary resistance which may contribute to the overshoot of the predicted boost ratio at resonance when compared to experimental data.

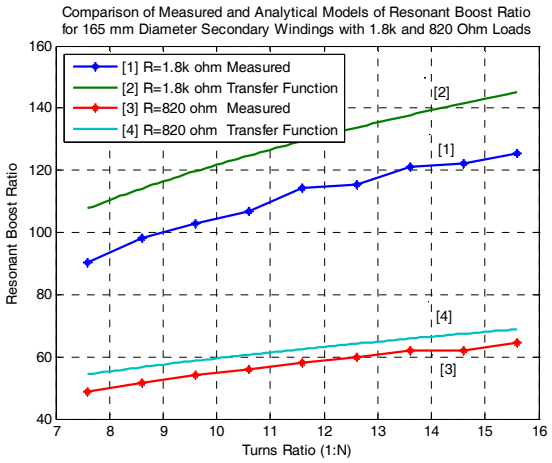

Figure 11. Measured and analytical models of boost ratio at resonance for varying turns ratio for the large core transformer.

The resonant frequency of a RLC circuit with the load resistance in parallel with the capacitance [16] is given in equation (3).

$$F_{res} = \frac{1}{2\pi}\sqrt{\frac{1}{L_{res}C_{res}} - \frac{1}{\left(R_{load}C_{res}\right)^2}} \qquad (3)$$

When the value of inductance from the Wheeler compensated area formula is used the predicted resonant frequency matches the measured value as seen in Figure 12.

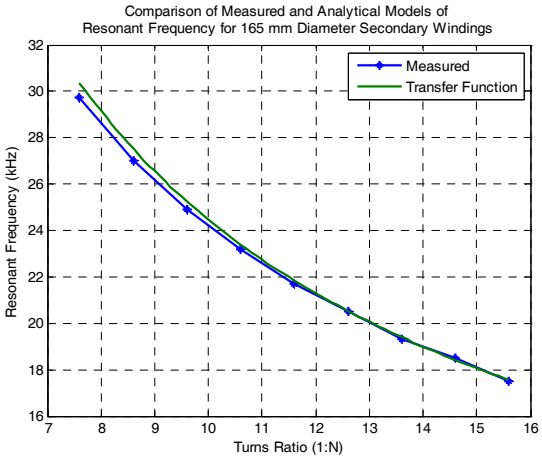

Figure 12. Measured and analytical models of resonant frequency as a function of turns ratio for the large core transformer.

As the load resistance is varied while the transformer is driven at resonant frequency, the boost ratio varies as shown in Figure 13. The transfer function model of the transformer accurately predicts the boost ratio over a wide range of load resistances. The knee at high load resistances is due to the finite resistance of the inductor limiting the maximum attainable boost ratio.

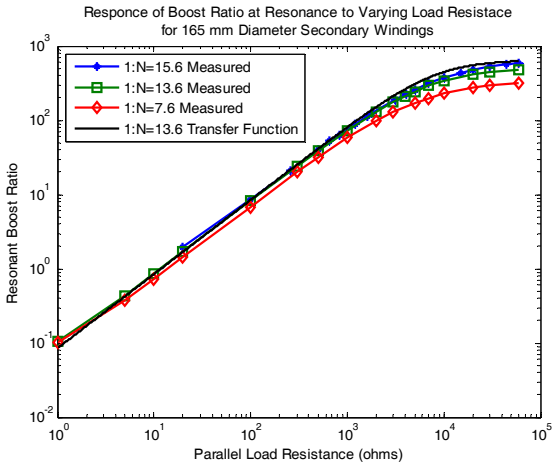

Figure 13. Measured and analytical models of boost ratio at resonance for varying load resistance for the large core transformer.

3.2 SMALL CORE TRANSFORMER TESTING

A small resonant transformer utilizing an amorphous "metglas" core, as shown in Figures 14 and 15, was constructed and tested to verify that the analytical formulas are not affected to any great extent by scaling of the transformer size. The secondaries consist of a parallel pair of 102 mm diameter windings with a secondary series resistance of 0.9 Ω for the 90 turn version. Further, two separate primaries, one with a 2.5 mΩ ESR, denoted "Low R" and the other with a 48 mOhm ESR, denoted "High R", as shown in Figure 16 were used to determine the effect of primary resistance on transformer performance.

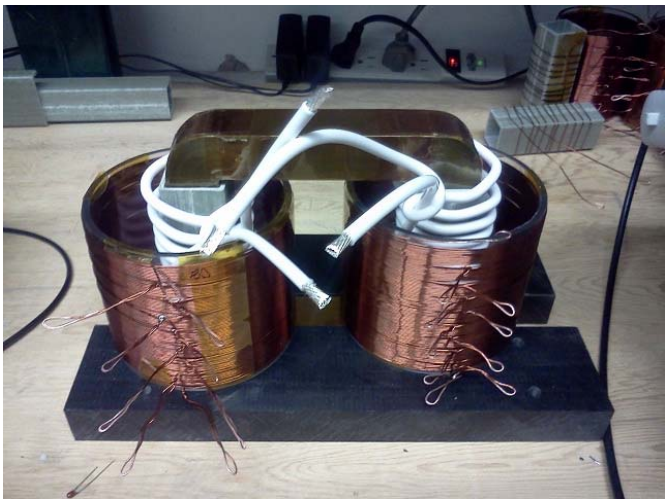

Figure 14. Small core resonant transformer.

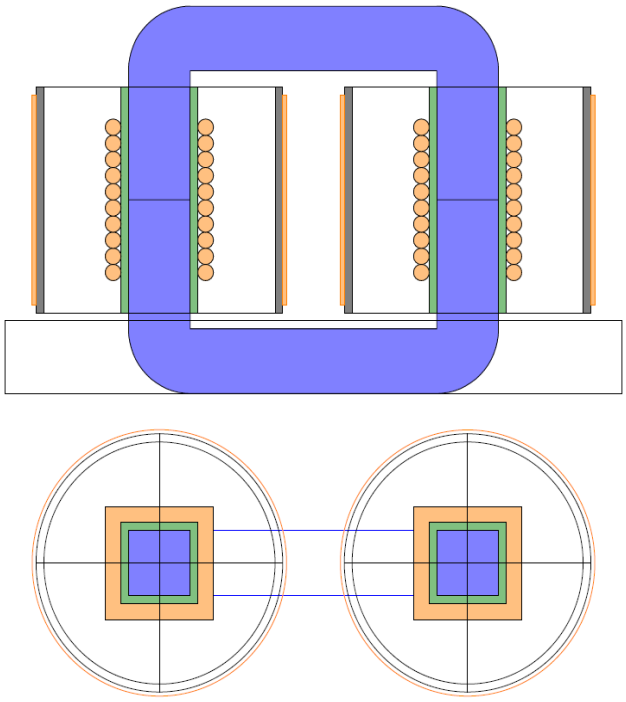

Figure 15. Small core resonant transformer assembly diagram.

Boost ratio for the small core transformer was measured for both Low R and High R primary windings. It was shown that the increase in primary resistance incurred by using a small gauge wire significantly degraded the performance of the resonant circuit, particularly for high turns ratios as shown in Figure 17.

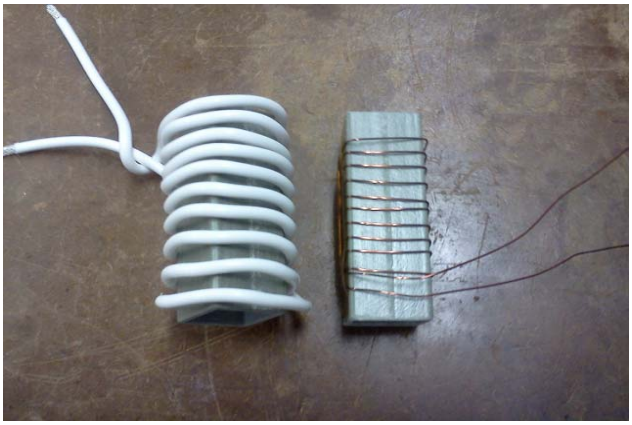

Figure 16. Low R and High R primary windings.

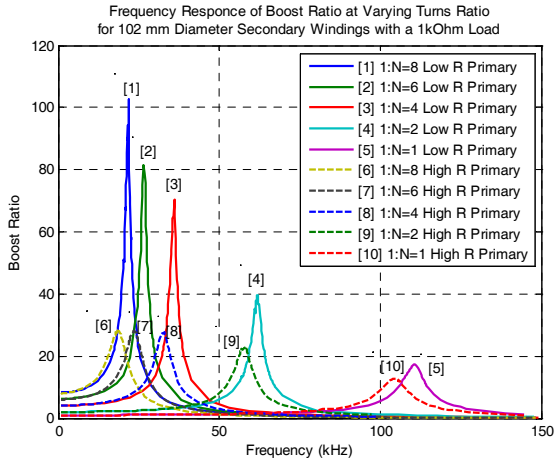

Figure 17. Boost ratio for the small core resonant transformer with a 1 k Ω load for Low R and High R primary windings.

While the analytical model accurately predicts leakage inductance for the low resistance Low R winding, the higher resistance High R winding diverges from the prediction particularly at high turns ratios as shown in Figure 18.

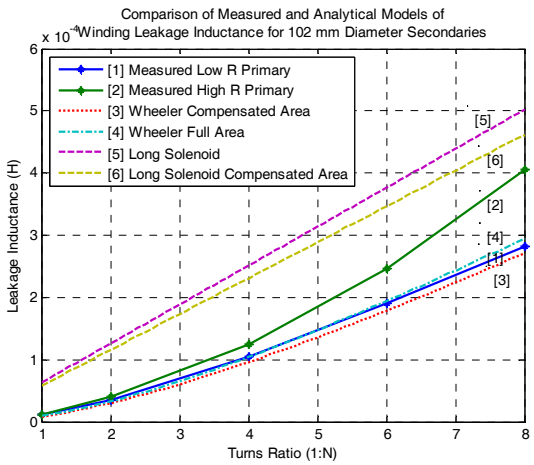

Figure 18. Measured and analytical models of secondary winding leakage inductance for the small core transformer.

The higher resistance primary greatly reduces the boost ratio, and increases secondary leakage inductance leading to a lower boost ratio and resonant frequency as shown in Figures 19 and 20. The higher effective leakage inductance is due to the higher resistance primary's inability to effectively screen magnetic flux from the secondary winding out of the transformer core. The current driven in the primary is dissipated by the resistance leading to a lower Q circuit and lower boost ratio at resonance. The high Q of the transformer with the Low R winding leads to difficulties measuring the peak boost ratio values, leading to the lower measured boost ratios for high turns ratios seen in Figure 20. Resonant frequency is measured and compared to the analytical model in Figure 21.

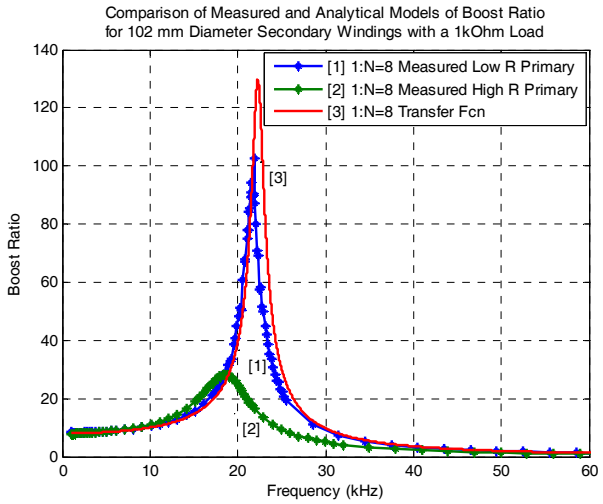

Figure 19. Measured and analytical models of boost ratio for the small core transformer with a 1k ohm load for Low R and High R primary windings.

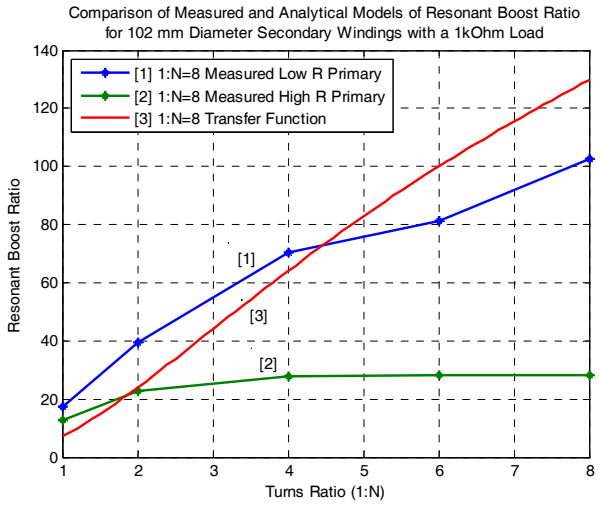

Figure 20. Measured and analytical models of boost ratio at resonance for varying turns ratio for the small core transformer.

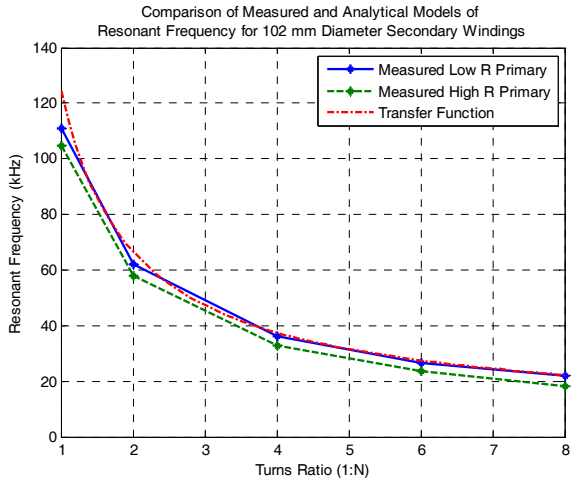

Figure 21. Measured and analytical models of resonant frequency as a function of turns ratio for the small core transformer.

4 DESIGN CONSIDERATIONS

When designing a high voltage resonant transformer, several considerations must be taken into account. At resonance the primary will be carrying a very large current at high frequency. For proper modeling and good performance of a resonant transformer, it is necessary to ensure low primary resistance to completely screen out privatized secondary magnetic flux from the core. The use of Litz wire on the primary, or independently insulated layered copper straps will decrease skin effect induced resistance at high frequencies and greatly improve performance.

For the analytical models presented herein, the DC resistance of the secondary is used and does not include skin effects or finite primary resistance which may contribute to the overshoot of the predicted boost ratio at resonance when compared to experimental data. The use of a low resistance primary will ensure accurate modeling of transformer performance.

5 CONCLUSION

The use of the analytical models presented in this paper will allow rapid design of loosely coupled transformers without the use of time consuming trial and error methods by providing accurate predictions of leakage inductance, resonant frequency, maximum boost ratio, and transfer function shape. For accurate modeling of resonant transformers and optimum performance, it is imperative to keep primary winding resistance low.

ACKNOWLEDGMENT

The authors thank Los Alamos National Lab for donating components to the project and William A Reass for developing the precedent of using resonant boost in klystron power supplies. This work is supported by the Department of Energy (DOE), USA.

REFERENCES

[1] W.A. Reass, D.M. Baca, R.F. Gribble, D.E. Anderson, J.S. Przybyla, R. Richardson, J.C. Clare, M.J. Bland and P.W. Wheeler, "High-Frequency Multimegawatt Polyphase Resonant Power Conditioning", IEEE Trans. Plasma Sci., Vol. 33, No. 4, pp.1210-1219, 2005.

[2] W.A. Reass, D.M. Baca, M.J. Bland, R.F. Gribble, H.J. Kwon, Y.S. Cho, D.I. Kim, J. McCarthy and K.B. Clark, "Operations of polyphase resonant converter-modulators at the Korean Atomic Energy Research Institute", IEEE Trans. Dielectr. Electr. Insul., Vol. 18, No. 4, pp. 1104-1110, 2011.

[3] W.A. Reass, J.D. Doss and R.F. Gribble, "A 1 megawatt polyphase boost converter-modulator for klystron pulse application", Pulsed Power Plasma Science (PPPS), Vol. 1, pp. 250–253, 2001.

[4] D.M. Divan and G. Skibinski, "Zero-switching-loss inverters for high-power applications", IEEE Trans. Industry App., Vol. 25, No. 4, pp. 634-643, 1989.

[5] G. Hua and F. C. Lee, "Soft-switching techniques in PWM converters," IEEE Trans. Indust. Electronics, Vol. 42, No. 6, pp. 595-603, 1995.

[6] M. J. Bland, J. C. Clare, P. Zanchetta, P.W. Wheeler and J.S. Pryzbyla, "A high frequency resonant power converter for high power RF applications", European Conf. Power Electronics and Applications, pp. P.1-P.10, 2005.

[7] W.A. Reass, D.M. Baca, J.D. Doss and R.F. Gribble, "Design technology of high-voltage multi-megawatt polyphase resonant converter modulators", IEEE Industrial Electronics Soc. (IECON), 29th Annual Conf., Vol. 1, pp.96-101, 2003.

[8] W.A. Reass, J.D. Doss, M.G. Fresquez, D.A. Miera, J.S. Mirabal and P. J. Tallerico, "A proof-of-principle power converter for the Spallation Neutron Source RF system", Particle Accelerator Conf., Vol. 1, pp. 426-428 1999

[9] W.A. Reass, D. L. Borovina, V.W. Brown, J.D. Doss, R.F. Gribble, T. W. Hardek, M.T. Lynch, D.E. Rees, P.J. Tallerico and D.E. Anderson, "The polyphase resonant converter modulator system for the Spallation Neutron Source linear accelerator", 25th Int'l. Power Modulator Sympos., pp. 684-688, 2002.

[10] D.E. Anderson, J. Hicks, M. Wezensky, D. Baca and W.A. Reass, "Operational Performance of the Spallation Neutron Source High Voltage Converter Modulator and System Enhancements", 27th Int'l. Power Modulator Sympos., pp. 427-430, 2006.

[11] O.H. Stielau and G.A. Covic, "Design of loosely coupled inductive power transfer systems", Int'l. Conf. Power System Technology (PowerCon), Vol. 1, pp. 85-90, 2000.

[12] Z.M. Shafik, K.H. Ahmed, S.J. Finney and B.W. Williams, "Nanocrystalline cored transformer design and implementation for a high current low voltage dc/dc converter", 5th IET Int'l. Conf. Power Electronics, Machines and Drives (PEMD), pp. 1-6, 19-21 2010.

[13] T. Filchev, F. Carastro, P. Wheeler and J. Clare, "High voltage high frequency power transformer for pulsed power application", 14th Int'l. Power Electronics and Motion Control Conf., pp. T6-165,T6-170, 2010

[14] S. Wei, W. Fei, D. Boroyevich and C.W. Tipton, "High-Density Nanocrystalline Core Transformer for High-Power High-Frequency Resonant Converter", IEEE Trans. Indust. Appl., Vol. 44, No. 1, pp. 213-222, 2008.

[15] H.A. Wheeler, "Formulas for the Skin Effect", Proc. IRE , Vol. 30, No. 9, pp. 412-424, 1942.

[16] K.L. Kaiser, *Electromagnetic Compatibility Handbook*, CRC Press, pp5.25-2.56, 2004.

Andrew H. Seltzman (M'12) was born in Raleigh, North Carolina in 1985. He received the B.S. degrees in physics and electrical engineering from the Georgia Institute of Technology, Atlanta, Georgia, USA in 2008, and the M.S. degree in electrical engineering from the University of Wisconsin, Madison, in 2012. He is currently at the University of Wisconsin, working on a Ph.D. in plasma physics with a focus on RF heating and current drive on Madison Symmetric Torus. Mr. Seltzman is a member of the American Physical Society, division of plasma physics.

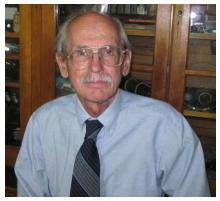

Paul D. Nonn began working at the University of Wisconsin as an undergrad student technician in 1961 on the first plasma experiment at UW, the linear quadrupole and continued through the evolution of three octopoles, culminating in the levitated octopole experiment focusing on pulsing radar magnetrons for unprecedented long pulses for ECH startup and developing HV pulsers. He subsequently worked in the nuclear engineering department on Phaedrus A, B and tokamak experiments until 1998. He worked for one year for Mik Physics on the development of a novel 100 kW plasma deposition power supply before returning to work at the University of Wisconsin. Since then he has worked on small aspect ratio tokamaks dealing with HV capacitor bank and high current circuitry design, finally returning to the physics department to develop the oscillating field current drive ignitron oscillator on Madison Symmetric Torus and the electron cyclotron heating klystron power supply.

Jay K. Anderson received the M.A. and Ph.D. degrees in physics and the M.S. in electrical and computer engineering from the University of Wisconsin, Madison. He has been a scientist at the University of Wisconsin for 15 years, primarily studying the physics of fusion relevant plasmas in the Madison Symmetric Torus. His primary interests are advanced control techniques of the reversed field pinch plasma, including heating and current drive by injection of neutral beams or microwaves. Dr. Anderson is a member of the American Physical Society, division of plasma physics.